

Evidence for Narrow Baryon Resonances in Inelastic pp Scattering

B. Tatischeff,¹ J. Yonnet,² N. Willis,¹ M. Boivin,² M. P. Comets,¹ P. Courtat,¹
R. Gacougnolle,¹ Y. Le Bornec,¹ E. Loireleux,¹ and F. Reide¹

¹*Institut de Physique Nucléaire, CNRS/IN2P3, F-91406 Orsay Cedex, France*

²*Laboratoire National Saturne, CEA/DSM CNRS/IN2P3, F-91191 Gif-sur-Yvette Cedex, France*

(Received 29 January 1997)

The reaction $pp \rightarrow p\pi^+N$ has been studied at three energies ($T_p = 1520, 1805, \text{ and } 2100 \text{ MeV}$) and six angles from 0° up to 17° (laboratory). Several narrow states have been observed in missing mass spectra at 1004, 1044, and 1094 MeV. Their widths are typically 1 order of magnitude smaller than the widths of N^* or Δ . Possible biases are discussed. These masses are in good agreement with those calculated within a simple phenomenological mass formula based on color magnetic interaction between two colored quark clusters. [S0031-9007(97)03686-7]

PACS numbers: 14.20.Gk, 12.40.Yx, 13.75.Cs, 14.20.Pt

The study of exotic hadrons (mesons and baryons) has been ongoing for several years, motivated by the possibility of relating these exotic states to multiquarks, hybrids, or glueballs. The experimental studies can be separated into two classes. The first class concerns studies of exotic mesons mainly, but also in a few cases of exotic baryons, with explicit exotic quantum numbers, or their exotic combinations. The second class of studies concerns low energy, narrow, exotic states with hidden exotic properties (strangeness or color, etc.) [1]. The main observable here is the small width of the observed structures. Even if such narrowness is not a firm signature [2], this is an essential characteristic from an experimental point of view. Some candidates with relatively large masses exist, and have been observed at Protvino, CERN, and Argonne, although the existence of some of them is still a subject of debate. The corresponding masses are above 1000 MeV for mesons and 1950 MeV for baryons. For experimental reasons (resolution and counting rates), nearly all results of low mass, narrow hadrons concern isovector dibaryons which are seen to be concentrated around certain values [3]. A number of authors have observed many candidates for such isovector narrow dibaryons. This mass spectrum agrees surprisingly well with a simple phenomenological mass formula [3] derived for two colored clusters in a diquark-quadrquark assumption inside an MIT (Massachusetts Institute of Technology) bag model. Different theoretical works have been performed on dibaryons. The first approaches within MIT spherical bags [4] have been improved using cloudy bags [5]. In these last calculations, dibaryons were found at masses close to 2.7 GeV. The same authors predict the existence of molecular states [2] in the lower mass region.

The experiment presented below is the study of the $pp \rightarrow p\pi^+N$ reaction. It was carried out using the proton beam at the Saturne Synchrotron and the SPES3 facility [6]. The incident proton energies were 1520, 1805, and 2100 MeV. The measurements were performed at six angles, for each energy, from 0° up to 17° [7].

The cryogenic H_2 target was 393 mg/cm^2 thick. Both particles, p and π^+ , were detected in coincidence in the solid angle of 10^{-2} sr ($\Delta\theta = \Delta\phi = \pm 50 \text{ mrd}$) of the magnetic spectrometer. The broad range of momenta studied by the detection, $600 < pc < 1400 \text{ MeV}$ at $B = 3.07 \text{ T}$, allowed the simultaneous study of a large range of missing masses ($939 < M_x < 1520 \text{ MeV}$). The particle trajectories were localized using drift chambers. The trigger consists of four planes of scintillating hodoscopes. Time of flight measurements over a distance of 3 m, in conjunction with energy loss measurements, allow the identification of the detected particles. Events were lost when both trajectories intersected on each plane of the detector. A simulation code describing the detector has been written in order to correct for such inefficiencies. These corrections, normalizing the data by a factor of ~ 1.25 , are smooth functions, except in a narrow range of $p\pi^+$ invariant masses corresponding to particles detected at the same position on the focal plane. Inside such an invariant mass range the data have been removed, since a peak on the correction function makes any eventual structure at the same mass doubtful.

The random coincidences and eventual wrong identification arising from $pp \rightarrow ppX$ events have been taken out using a second time of flight between both particles. The total coincidence window, common to all time of flight channels, was $\pm 2 \text{ ns}$. Since certain events from a $pp \rightarrow ppX$ reaction can simulate real $pp \rightarrow p\pi^+X$ events, checks were carried out to ensure that their contribution is small. They are randomly distributed in the two-dimensional plot of invariant mass against missing mass. In a very small number of cases (0.6% of events), the data reduction code makes a wrong assignment between trigger and chamber informations. These events have been removed.

The necessary conditions required for narrow and small structures study were fulfilled in this experiment. These are (i) a good mass resolution; the σ on missing mass increases from 2.5 up to 9.4 MeV for spectrometer angles

varying from 0° up to 17° , (ii) high statistics ($\geq 10^3$ events per channel), (iii) good particle identification, and (iv) studies in different kinematical conditions in order to check the mass stability of eventual narrow structures, from data obtained at different angles and incident energies.

The $p\pi^+$ invariant mass versus the missing mass of events (before normalization) obtained at 1805 MeV, 0.75° is presented in Fig. 1. The limits of the plot correspond to the lower and upper spectrometer acceptance limits of 600 and 1400 MeV/c, respectively. The empty zone corresponds to the points of intersection of two trajectories on focal plane, where the first drift chamber was located. No other empty (intense) line appears which would correspond to the dead (hot) region in this chamber. The neutron peak is clearly seen on the left side of Fig. 1. It corresponds to events produced with a Δ in invariant mass, partly cut when they lie outside the acceptance, and above, heavier Δ and $p\pi^+$ phase space events. The region with a large population of events at $M_x \sim 1220$ MeV, $M_{p\pi^+} \sim 1200$ MeV corresponds to the double delta production, Δ^0 and Δ^{++} , respectively, in missing mass and invariant mass. Some weakly excited vertical lines appear in the region $1000 < M_x < 1100$ MeV.

Figure 2 shows the result of the projection of the previous two-dimensional plot normalized to constant

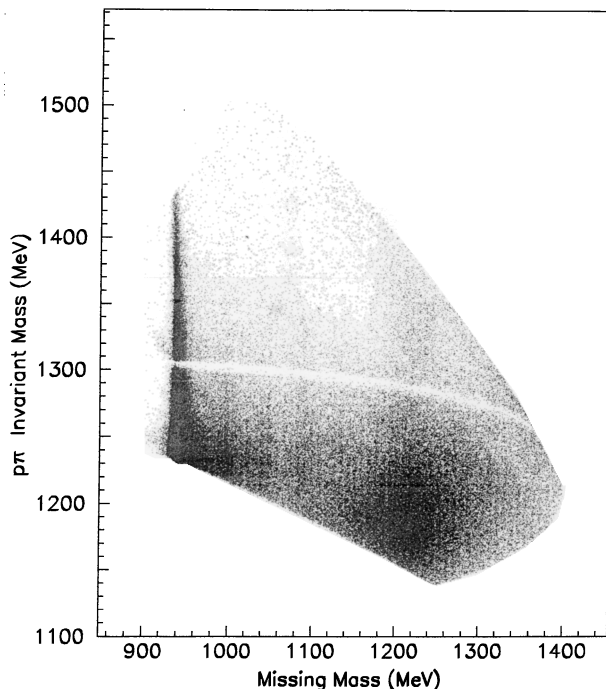


FIG. 1. Two-dimensional plot at 1805 MeV proton energy and 0.75° for the mean value of the two detected particles. The data exhibit clearly the production of delta neutron and two deltas events, and between them an indication of some narrow and small structures.

$\Delta p_p \cdot \Delta p_\pi$ and the same data for the three lowest angles at 1520 and 1805 MeV, selected for missing masses larger than 960 MeV, in order to set off the narrow structures. The decrease of the cross sections and the broadening of the resolution explain why the structures vanish at large angles. The weakly excited lines seen in Fig. 1 are clearly identified in Fig. 2. Empty target measurements have been performed for the same number of incident protons. A low level count rate ($< 5\%$) and a flat distribution (without structure) have been observed for the empty target runs.

A careful study has been undertaken in order to make sure that the structures were not produced by events from the $pp \rightarrow p\pi^+n$ reaction, with the p or π^+ emitted at large vertical angles, which fall outside the useful solid angle acceptance. This could arise for events having a momentum larger than 1400 MeV/c, then slowed down by the lead slits and stainless steel rings at the entrance of the spectrometer. Such an eventuality has been introduced in the simulation code, and shows a small, smooth contribution up to 1060 MeV with a peak arising at masses above and broader than the observed structures. At the missing mass of 1004 (1044) MeV, where the first (second) structure has been observed, the effect of the slits and stainless steel rings is small and varies monotonically with the mass (see

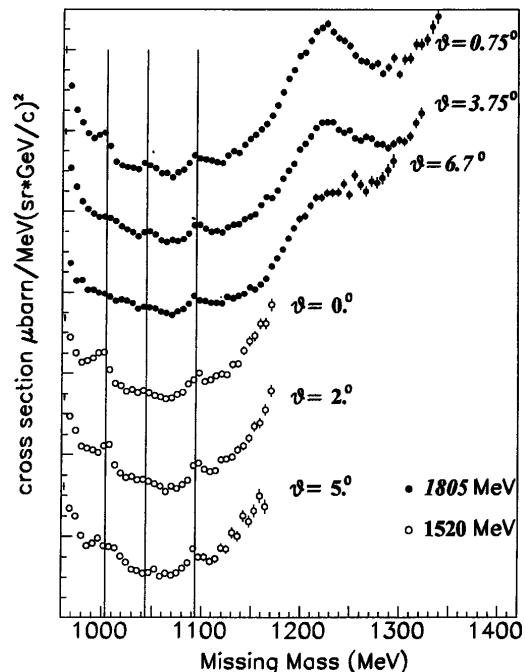


FIG. 2. Missing mass differential cross-sections for the $pp \rightarrow p\pi^+X$ reaction for the three lowest angles at $T_p = 1520$ and 1805 MeV, selected for missing masses larger than 960 MeV. Data have been binned into 5.6 MeV mass intervals, shifted and amplified in order to allow the presentation of all six angles inside the same figure. Vertical lines indicate the mean position of the structures.

TABLE I. Narrow structure cross sections laboratory in $\mu\text{b}/(\text{sr GeV}/c)^2$, absolute errors, widths (σ) and number of standard deviations (S.D.).

M_x (MeV)	T_p (MeV)	Angle	Cross sec. (err.)	Width (MeV)	S.D.	
1004	1520	0°	271(42)	5	5.9	
		2°	260(29)	5	8.6	
		5°	223(34)	12	3.6	
		17°	observed			
1044	1520	5°	59(27)	4	2	
		17°	observed			
		1805	0.75°	144(15)	5	9.1
1094	1520	0.75°	120(23)	7	5.1	
		3.75°	606(178)	4	2.9	
	1805	1520	5°	59(27)	4	2
			17°	observed		
			0.75°	144(15)	5	9.1
			3.75°	95(18)	5	5.1
	2100	1520	6.7°	59(14)	8	4.1
			13°	observed		
			0.3°	560(87)	10	6.2
			3°	631(72)	15	6.1
1805			0.75°	253(20)	8	11.6
3.75°			261(23)	8	10.6	
1094	1520	0°	231(44)	7	5	
		2°	212(44)	5	4.3	
		5°	112(39)	4	2.4	
		9°	97(29)	8	3.1	
	1805	1520	0.75°	253(20)	8	11.6
			3.75°	261(23)	8	10.6
			6.7°	81(16)	5	4.8
			9°	37(10)	6	3.5
2100	1520	0.3°	251(49)	7	4.7	
		3°	223(45)	7	4.1	

[8] for a more detailed discussion). We conclude therefore that there is no contamination in the 1004 and 1044 MeV structures, however, a doubt remains around 1094 MeV.

The cross sections of these structures have been extracted, using polynomial fits for the background and Gaussians for the peaks. The mass structures are well

defined, but their cross sections and widths are not well defined. They depend heavily on the shape of the background and on the experimental resolution. Table I summarizes these results. The laboratory cross sections have been normalized to constant momenta ranges. An overall systematic error of 20% can be estimated and is mainly due to the large background subtraction uncertainties.

Although many experiments devoted to various other studies have explored the baryonic excitation function between the nucleon and delta, and have often observed some shoulders or discontinuities in that region, none of them were accurate enough in order to be able to ascertain the real presence of new states. A (not exhaustive) list of such experiments is presented in Table II.

As pointed out before, narrow baryons, which are sometimes still a subject of debate, have already been observed in different laboratories. They appear as candidates for exotic baryons with hidden strangeness in invariant masses of strange baryons and strange mesons [22–25].

Although it is not proven that these structures are a manifestation of colored quark clusters, we have considered such an assumption. The mass formula for two clusters of quarks at the ends of a stretched bag was derived some years ago in terms of color magnetic interactions [4,26];

$$M = M_0 + M_1[i_1(i_1 + 1) + i_2(i_2 + 1) + (1/3)s_1(s_1 + 1) + (1/3)s_2(s_2 + 1)], \quad (1)$$

where M_0 and M_1 are parameters deduced from mesonic and baryonic mass spectra and $i_1(i_2)$ and $s_1(s_2)$ are isospin and spin of the first and second quark cluster, respectively. We make the assumption that the clusters are $q^2 - q$ or $(q\bar{q})^2 - q^3$. The spin (isospin) values for a diquark ($q\bar{q}$) cluster are 0 or 1 and for a three quark cluster 1/2 or 3/2. Since the masses correspond to zero radial excitation, all parities are positive.

TABLE II. Experiments having studied the baryonic mass region between nucleon and delta.

Particles	Accelerator	Reaction	Reference	
nucleons	LAMPF	$np \rightarrow pX$ (0°)	B. E. Bonner <i>et al.</i> (1983) [9]	
		$pp \rightarrow p\pi^+n$ (800 MeV)	A. D. Hancock <i>et al.</i> (1983) [10]	
	Saturne	$pp \rightarrow p\pi^+n$ (800 MeV)	J. Hudomalj-G. <i>et al.</i> (1978) [11]	
		$p(^3\text{He}, t)X$	D. Contardo <i>et al.</i> (1986) [12]	
photons	MAMI	$^3\text{He}(p, t)X$	B. Tatischeff <i>et al.</i> (1978) [13]	
		$np \rightarrow pX$	G. Bizard <i>et al.</i> (1976) [14]	
		$\gamma p \rightarrow \pi^0 X$	M. Fuchs <i>et al.</i> (1996) [15]	
		$\gamma p \rightarrow \gamma X$ (90°)	C. Molinari <i>et al.</i> (1996) [16]	
	Saskatchewan Brookhaven Saclay-ALS Bonn		$\gamma p \rightarrow p\pi^+\pi^-$	A. Braghieri <i>et al.</i> (1995) [17]
			$\gamma p \rightarrow p\pi^0\pi^0$	"
			$\gamma n \rightarrow p\pi^+\pi^0$	"
			$\gamma p \rightarrow \gamma X$	E. L. Hallin <i>et al.</i> (1993) [18]
		$\gamma p \rightarrow \pi^0 X$	G. Blanpied <i>et al.</i> (1992) [19]	
		$\gamma p \rightarrow \pi^0 X$	E. Mazzucato <i>et al.</i> (1986) [20]	
		$\gamma d \rightarrow pX$	J. Arends <i>et al.</i> (1996) [21]	

Experimental BARYONIC MASSES (MeV) Calculated

Spin	Isospin	Mass	Mass	Spin	Isospin		
1/2	N(P ₁₁)	1/2 1440.	1440.	1/2...7/2	1/2,3/2		
			1407.	3/2,5/2	3/2		
				1/2	1/2...5/2		
				5/2	3/2		
					1/2,3/2		
				1340.	3/2,5/2	1/2,3/2	
				1306.	3/2	3/2	
					1/2,3/2	3/2	
					1/2...5/2	1/2,3/2	
				1273.	3/2...7/2	1/2	
3/2	Δ	3/2 1232.	1239.	1/2...7/2	1/2		
			1206.	1/2	3/2		
				3/2	1/2,3/2		
				1/2,3/2	1/2,3/2		
				1139.	3/2,5/2	1/2	
				1106.	1/2	1/2,3/2	
					1/2...5/2	1/2	
				(1094.)			
				1044.	1039.	3/2	1/2
				1004.	1005.	1/2,3/2	1/2
1/2	N	1/2 939.	939.	1/2	1/2		

FIG. 3. Baryonic experimental and calculated masses.

In order to define the two parameters, we first assume that the nucleon mass is obtained when $i_1 = s_1 = 0$, and $i_2 = s_2 = 1/2$, giving therefore the nucleon quantum numbers $S = I = 1/2$. We assume also that the Roper resonance at 1440 MeV (the first excited state of the nucleon) is obtained with $i_1 = 1, s_1 = 0, i_2 = 3/2$, and $s_2 = 1/2$ giving, among degeneracy, possible experimental quantum numbers $S = I = 1/2$. Such assumptions allow us to predict the masses of the two first possible $S = I = 3/2$ states at 1206 ($i_1 = s_1 = 1$ and $i_2 = s_2 = 1/2$) and 1239 MeV ($i_1 = 1, s_1 = 0, i_2 = 1/2$, and $s_2 = 3/2$), close to the mass of the first delta resonance. Such assumptions determine the values of $M_0 = 838.2$ MeV and $M_1 = 100.3$ MeV. The corresponding mass spectra obtained using relation (1) without any adjustable parameter, is shown in Fig. 3. As in the case of narrow isovector dibaryons [3], a good agreement is observed between the experimental and calculated masses. Masses, spins, and isospins for additional levels are predicted, and often have several possible spin and isospin values due to the degeneracy mentioned above. It is not excluded that more precise experiments will, in the future, observe these levels. Below the pion emission thresholds, 1075 MeV for baryons and 2012 MeV for dibaryons, the only possible decay channel is the radiative one. Below and above the pion emission thresholds, the assumption that they are states of two colored quark clus-

ters gives a good agreement between the color magnetic mass formula and the experimental observations.

In conclusion, three narrow baryonic states have been observed at the following masses: 1004, 1044 MeV, and with a smaller confidence at 1094 MeV, without any anomalous experimental behavior. The latter state is only 19 MeV above the pion threshold mass. The widths of each of these three observed states are probably in the range 4–15 MeV. Such narrow widths are consistent with the need for radiative decay of the two lowest mass structures, and with the small phase space for the strong decay of the third.

- [1] L. G. Landsberg, Phys. At. Nucl. **27**, 42 (1994).
- [2] E. L. Lomon, in Proceedings of the XIIIth International Seminar on High Energy Physics Problems, Dubna, 1996 (to be published).
- [3] B. Tatischeff, in Proceedings of the XIIth International Seminar on High Energy Physics Problems, Dubna, 1994 (to be published).
- [4] P. J. Mulders, A. T. Aerts, and J. J. de Swart, Phys. Rev. D **21**, 2653 (1980); Phys. Rev. D **19**, 2635 (1979); Phys. Rev. Lett. **40**, 1543 (1978).
- [5] P. LaFrance and E. L. Lomon, Phys. Rev. D **34**, 1341 (1986); P. Gonzalez, P. LaFrance, and E. L. Lomon, Phys. Rev. D **35**, 2142 (1987).
- [6] M. P. Comets *et al.*, Report No. IPNO DRE 88-41.
- [7] Only three angles at 2100 MeV: 0.7°, 3°, and 9°.
- [8] B. Tatischeff and J. Yonnet, in Proceedings of the XIIIth International Seminar on High Energy Physics Problems, Dubna, 1996 (Ref. [2]).
- [9] B. E. Bonner *et al.*, Phys. Rev. D **27**, 497 (1983).
- [10] A. D. Hancock *et al.*, Phys. Rev. C **27**, 2742 (1983).
- [11] J. Hudomalj-Gabitzch *et al.*, Phys. Rev. C **18**, 2666 (1978).
- [12] D. Contardo *et al.*, Phys. Lett. **168B**, 331 (1986).
- [13] B. Tatischeff *et al.*, Phys. Lett. **77B**, 254 (1978).
- [14] G. Bizard *et al.*, Nucl. Phys. **B108**, 189 (1976).
- [15] M. Fuchs *et al.*, Phys. Lett. B **368**, 20 (1996); V. Bernard, N. Kaiser, and Ulf-G. Meissner, Phys. Lett. **B378**, 337 (1996).
- [16] C. Molinari *et al.*, Phys. Lett. B **371**, 181 (1996).
- [17] A. Braghieri *et al.*, Few-Body Syst. Suppl. **8**, 171 (1995).
- [18] E. L. Hallin *et al.*, Phys. Rev. C **48**, 1497 (1993).
- [19] G. Blanpied *et al.*, Phys. Rev. Lett. **69**, 1880 (1992).
- [20] E. Mazzucato *et al.*, Phys. Rev. Lett. **57**, 3144 (1986).
- [21] J. Arends *et al.*, Nucl. Phys. **A412**, 509 (1984).
- [22] S. V. Golovkin *et al.*, Z. Phys. C **68**, 585 (1995); Phys. At. Nucl. **58**, 1342 (1995).
- [23] A. N. Aleev *et al.*, Z. Phys. C **25**, 205 (1984).
- [24] V. M. Karnaukhov, C. Coca, and V. I. Moroz, Phys. At. Nucl. **58**, 796 (1995).
- [25] J. Amirzadeh *et al.*, Phys. Lett. **B89**, 125 (1979).
- [26] C. Besliu, L. Popa, and V. Popa, J. Phys. G **18**, 807 (1992).